

Metal Coordination and Mechanism of Multicopper Nitrite Reductase

SHINNICHIRO SUZUKI,*
KUNISHIGE KATAOKA, AND
KAZUYA YAMAGUCHI

Department of Chemistry, Graduate School of Science,
Osaka University, Toyonaka, Osaka 560-0043, Japan

Received October 19, 1999

ABSTRACT

Cu-containing nitrite reductase is a homotrimer in which a ca. 36 kDa monomer contains each of type 1 Cu (two His, Cys, and Met ligands) and type 2 Cu (three His and solvent ligands). Type 1 Cu receives one electron from an electron donor and transfers it to the reaction center, type 2 Cu. The distance between the two Cu atoms bound by the Cys-His sequence segment is 12.6 Å. The intramolecular electron transfer from type 1 Cu to type 2 Cu occurs probably through this segment. The noncoordinated Asp and His residues around type 2 Cu play important roles in both the electron-transfer and the catalytic processes.

Introduction

Organic nitrogen as a constituent part of the cell is required for all organisms. As shown in Figure 1, the terrestrial inorganic nitrogen cycle sustained by bacteria plays an important role in the other organisms, animals, and plants. The cycle manifests the redox chemistry inherent to the principal inorganic nitrogen species, dinitrogen (N^0), ammonia (N^{-III}), and nitrate (N^{+V}). Inorganic nitrogen is introduced into the biosphere by biological fixation process of dinitrogen and removed from there again by denitrification. Therefore, the nitrogen cycle has received much attention in recent years because of its ecological importance. That is to say, the unbalance of the nitrogen cycle brings about serious problems for all organisms on the earth. For example, it has been reported that feeding humankind demands so much nitrogen-based fertilizer that the distribution of nitrogen compounds on the earth has been changed in dramatic, and sometimes dangerous, ways.¹

Denitrification is the dissimilatory reduction of nitrate or nitrite to produce dinitrogen by prokaryotic organisms (Figure 1): it is part of the bioenergetic apparatus of the

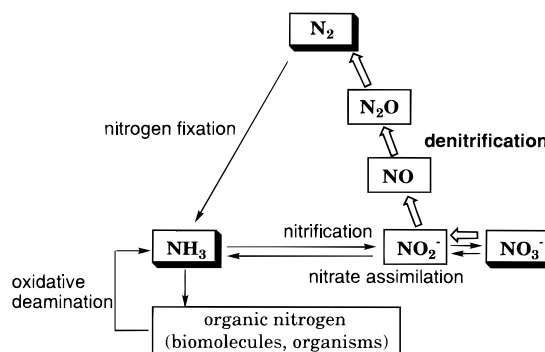


FIGURE 1. Biogeochemical nitrogen cycle on the earth.

cell of which denitrifying bacteria occupy a wide range of natural habitats including soil and water, and return a large amount of fixed nitrogen to the atmosphere. The denitrification is a cascade of anaerobic respiration processes catalyzed by the corresponding metalloenzymes.^{2,3} The first step (nitrate (N^{+V}) \rightarrow nitrite (N^{+III}), two-electron reduction) is carried out by dissimilatory membrane-bound nitrate reductase containing molybdenum with both heme and non-heme irons, which has an Mo(VI)O center with two dithiolene-containing pterin cofactor ligands.⁴ The second step (nitrite (N^{+III}) \rightarrow nitrogen monoxide (N^{+II}), one-electron reduction) is catalyzed by the dissimilatory soluble enzyme, nitrite reductase (NIR), of which two distinct types have so far been known: multi-heme NIR and multi-copper NIR (CuNIR). Heme-containing NIR is a 120 kDa homodimer, in which each monomer carries one heme *c* and one heme *d*.^{5–7} CuNIR is a 110 kDa homotrimer, in which a monomer contains each of type 1 Cu (blue copper) and type 2 Cu (nonblue copper).^{8–16} In the third step (nitrogen monoxide ($2N^{+II}$) \rightarrow nitrous oxide ($2N^{+I}$), two-electron reduction), nitric oxide reductase containing hemes *b* and *c* is concerned.^{2,3} This membrane-bound enzyme consists of two polypeptides of 42 and 20 kDa associated with two hemes *b* and one heme *c*, respectively.¹⁷ The final step (nitrous oxide ($2N^{+I}$) \rightarrow dinitrogen ($2N^0$), two-electron reduction) is carried out by a soluble copper enzyme, nitrous oxide reductase. The oxidized enzyme appears bright purple or pink and changes into typical blue expected for copper proteins after the reduction with dithionite.² According to the recent X-ray crystal structure analysis of *Pseudomonas nautica* nitrous oxide reductase,¹⁸ the enzyme is a homodimer, and a monomer (ca. 65 kDa) contains a Cu_A electron entry site (thiolate-bridged, binuclear copper site), similar to that in cytochrome *c* oxidase,^{19,20} and a Cu_Z catalytic center. The Cu_Z center is a new type of metal cluster, in which four Cu atoms are ligated by seven His residues.

Dissimilatory nitrite reductase is the key enzyme of denitrification in catalyzing the first committed step that leads to a gaseous intermediate. This paper will focus on the structural and functional aspects of type 1 Cu and type

Shinnichiro Suzuki is Professor of Chemistry at Osaka University. He received a B.S. degree from Tokyo Metropolitan University in 1969 and a Ph.D. from Osaka University in 1974. His research interests are in the area of bioinorganic chemistry of metalloproteins.

Kunishige Kataoka is a research associate at Osaka University. He received a B.S. degree from Tsukuba University in 1987 and a Ph.D. from Osaka University in 1995.

Kazuya Yamaguchi is a research associate at Osaka University in Japan. He earned his B.S. degree from Shizuoka University in 1987 and his Ph.D. in chemistry from Kyoto University in 1992.

* Corresponding author. Fax: +81-6-6850-5785. E-mail: bic@ch.wani.osaka-u.ac.jp.

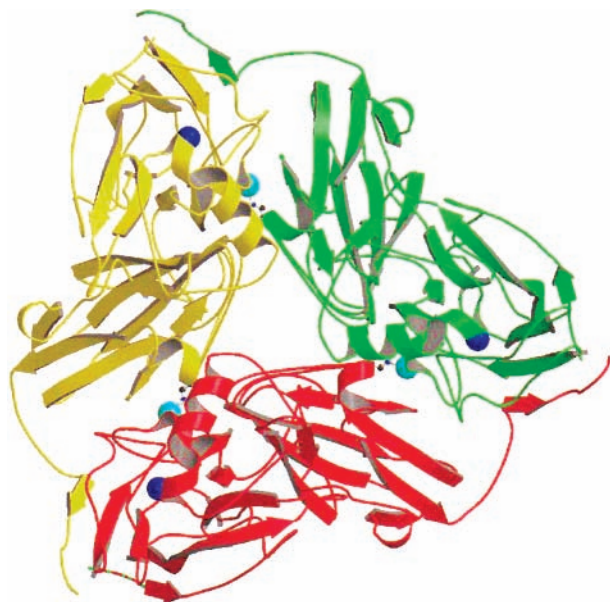


FIGURE 2. Homotrimer structure of blue AxxNIR. Dark blue and light blue spheres are type 1 Cu and type 2 Cu, respectively.

2 Cu in blue and green CuNIRs, which are typical of CuNIRs classified by spectroscopic properties of type 1 Cu.²¹ The blue CuNIRs from *Alcaligenes xylosoxidans* NCIB 11015 (AxxNIR)^{22–24} and *Alcaligenes xylosoxidans* GIFU 1051 (AxxNIR)²⁵ exhibit an intense 593-nm absorption band ($\epsilon = 3800 \text{ M}^{-1} \text{ cm}^{-1}$) due to a S(Cys) \rightarrow Cu(II) charge-transfer transition of type 1 Cu. The enzymes show EPR signals of type 1 Cu with axial symmetry such as those of electron-transfer blue copper proteins (cupredoxins), plastocyanin and azurin. The green CuNIRs isolated from *Achromobacter cycloclastes* IAM 1013 (AciNIR)^{26–29} and *Alcaligenes faecalis* S-6 (AfsNIR)³⁰ display two intense visible absorption bands (AciNIR, 460 nm ($\epsilon = 2400$) and 584 nm ($\epsilon = 1800 \text{ M}^{-1} \text{ cm}^{-1}$))²⁵ and rhombic EPR signals of type 1 Cu. Two intense visible absorption bands are also assigned to S(Cys) \rightarrow Cu(II) transfer transitions of type 1 Cu.³¹

Structure of CuNIR

The protein sequence of AxxNIR composed of 360 amino acid residues is perfectly identical to that of AxxNIR,³² but the difference between open reading frames of these NIRs is only one base in the total 1083 bp gene sequence.³³ AxxNIR shows a high level of homology (ca. 80%) with the other blue NIR from *Pseudomonas aureofaciens*³⁴ and has ca. 70% identity with green AciNIR and AfsNIR.²¹

The X-ray crystal structure of green AciNIR was reported for the first time by Godden et al.⁸ The crystal structures of two green NIRs (AciNIR^{8,11} and AfsNIR^{9,10,13}) and two blue NIRs (AxxNIR^{12,15,16} and AxxNIR¹⁴) have so far been analyzed. All of these enzymes have quite similar whole structures, regardless of the colors of NIRs. Three identical subunits are tightly associated around a 3-fold axis to form a trimer around a central channel of 5–6 Å, as illustrated in Figure 2. The type 1 Cu site is bound in one subunit, but the type 2 Cu site is located between two subunits. The type 2 Cu site is bound by two His

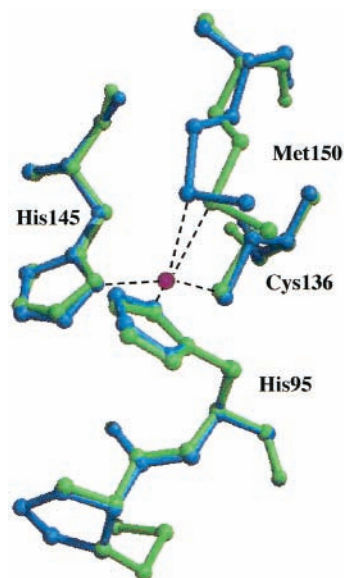


FIGURE 3. Superposition of type 1 Cu sites of oxidized AxxNIR (blue) and AfsNIR (green). The numbers refer to the AciNIR sequence.

residues from a monomer and one His from an adjacent monomer. The interatomic distance between the two Cu sites is 12.6 Å. The polypeptide fold forms two domains of which each consists predominantly of an eight-stranded β -barrel like cupredoxins. The core regions of the two β -barrels superimpose with a root mean square deviation of 1.25 Å on the C(α) atoms.^{15b} In a monomer, two β -barrels are stacked on each other, and there are one long and two short α -helical regions.

The type 1 Cu(II) sites of blue AxxNIR and green AfsNIR are shown in Figure 3.¹⁴ The superposition of the two sites was carried out on the three strong ligands, His95N(δ 1), His145N(δ 1) (Cu–N = 2.00–2.11 Å), and Cys136S(γ) (Cu–S = 2.08–2.18 Å).^{13,14} The fourth weak ligand is Met150 (Cu–S = 2.62–2.64 Å). In AxxNIR, the displacement of the Cu atom out of the NNS plane defined by 2N(His) and S(Cys) atoms toward S(Met150) is ca. 0.5 Å, like that in AfsNIR. The S(Met) ligand of AxxNIR deviates slightly from the axial position of the NNS plane, whereas that of AfsNIR is in the considerably tilted position. These Cu(II)–S(Met) distances are shorter than that of plastocyanin by ca. 0.2 Å. Therefore, the geometries of the type 1 Cu sites in blue NIR (AxxNIR and AxxNIR) and green NIR (AfsNIR and AciNIR) are distorted tetrahedral and flattened tetrahedral, respectively. The imidazole ring of His145 bound to type 1 Cu with the N(δ 1) atom is oriented such that the N(ϵ 2) atom is exposed to the solvent at the bottom of a small cavity composed of hydrophobic amino acid residues (Met, Trp, and Pro) in the protein surface. Surrounding the cavity containing His145 is a flat area of protein surface, with the Cu atom being ca. 7 Å beneath. The intermolecular electron transfer from a donor protein to the type 1 Cu(II) site might occur through the cavity.

Type 2 Cu bound at the interface of two subunits lies at the bottom of a 12–13 Å deep solvent channel, being the substrate-binding and reduction site. The His135–Cys136 amino acid sequence segment bound to type 2 Cu with His135 is also bound to type 1 Cu with Cys136,

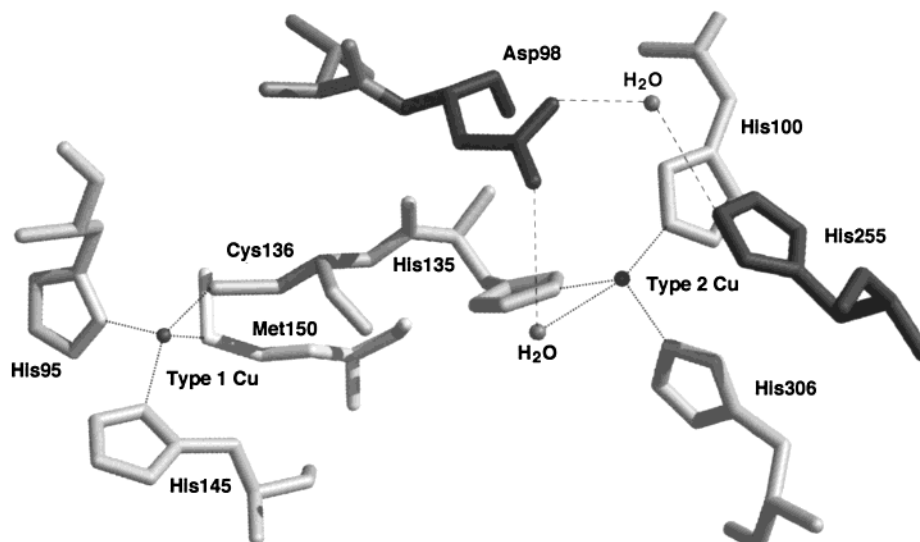


FIGURE 4. Type 1 and type 2 Cu sites in oxidized AxxNIR. The numbers refer to the AxiNIR sequence. His306 residue comes from an adjacent subunit.

as shown in Figure 4. The type 2 Cu center is ligated by three His ligands (His100 N(ϵ 2), His135 N(ϵ 2), and His306 N(ϵ 2)). In the early reports, the total number of Cu atoms per one subunit fluctuated,^{22,25,28,29} indicating type 2 Cu would be partially or considerably removed under drastic conditions such as the enzyme preparation. The three His ligands together with a solvent ligand (H₂O or OH⁻) form a distorted tetrahedral geometry. All the His residues remain oriented in the same place even on selective removal of type 2 Cu.¹¹

In Figure 4, there is a hydrogen-bonding network extending from the solvent ligand of type 2 Cu, which involves both the Asp98 and His255 residues in the vicinity of the Cu atom.^{11,13–15} The solvent ligand is hydrogen bonded to the carboxylate group of Asp98, which in turn forms a H₂O-bridged hydrogen bond to the imidazole nitrogen atom of His255. X-ray crystal structure analyses of nitrite-soaked oxidized NIRs showed that nitrite is coordinated to type 2 Cu(II) in an asymmetric bidentate fashion through two oxygen atoms (Cu–O = 2.2 and 2.3 Å in AfsNIR;¹³ 1.65 and 2.65 Å in AxxNIR^{15b}) instead of the solvent ligand. One of the nitrite oxygens forms a hydrogen bond to one of the carboxylate oxygen atoms of Asp98. The other carboxylate oxygen atom of Asp98 also forms a H₂O-bridged hydrogen bond to His255, as observed in the vicinity of the type 2 Cu site with the solvent ligand. In colorless reduced AfsNIR, there is no solvent ligand (H₂O or OH⁻) at the type 2 Cu(I) site, although the structure of the type 1 Cu site is scarcely changed.¹³ The type 2 Cu(I) site, having three His ligands, results in a tricoordinate tetrahedral geometry. The X-ray crystal structures around the type 2 Cu site will give an important clue to the mechanism of nitrite reduction.

Intermolecular Electron-Transfer Process of CuNIR

For nitrite reduction, NIR requires one electron from an electron donor protein. Electron donors for green AxiNIR^{27,35}

and AfsNIR³⁶ are a cupredoxin, pseudoazurin (pAz) isolated with the cognate NIR. pAz (ca. 14 kDa) shows an intense ca. 590-nm band with two weak bands around 450 and 780 nm, and a rhombic EPR signal.³⁷ The second-order rate constant of the electron-transfer reaction from Axi-pAz (pI = 8.6, $E_{1/2}$ = +0.26 V vs NHE at pH 7.0)³⁷ to AxiNIR (pI = 4.6, $E_{1/2}$ (type 1 Cu) = +0.24 V vs NHE at pH 7.0)²⁵ is $7.3 \times 10^5 \text{ M}^{-1} \text{ s}^{-1}$ at pH 7.0 and 20 °C.^{21,38}

The overall topologies of the pAz's from *Alcaligenes faecalis* S-6 (Afs-pAz)³⁹ and *Achromobacter cycloclastes* (Axi-pAz)⁴⁰ consist of an eight-stranded β -barrel like those of plastocyanin and azurin. The distorted tetrahedral copper site bound by His40, His81, Cys78, and Met86 is located below the protein surface at a depth of ca. 5 Å. Nine of a total 13 Lys residues surround the hydrophobic patch of the molecule, from which the His81 ligand protrudes slightly. Afs-pAz has a surface ring of four Lys residues around the Cu center (the 10–13 Å distances between the N ζ atoms of the Lys side chains and the Cu atom).^{36,41} There is little change in the k_{cat} values of intermolecular electron transfer on replacement of these Lys residues with Ala, but the K_{m} values increase by a factor of 2–3.³⁶ These findings suggest that pAz interacts with NIR through the domain containing these Lys residues close to the Cu center. At the AfsNIR surface around the type 1 Cu site, three Glu and Asp residues are substantially conserved in green NIRs. The substitution of Ala for these acidic amino acid residues decreases in k_{cat} and increases in K_{m} , suggesting that these negatively charged residues are involved in electrostatic interaction with pAz.⁴¹ The recent surface charge calculations of AxxNIR and AfsNIR have demonstrated that a surface charge distribution for AfsNIR is almost exclusively negative, but for AxxNIR, the surface charge is much more neutral.^{15b}

Azurin (Az; ca. 14 kDa) is a cupredoxin isolated with blue AxxNIR and AxxNIR, exhibiting an intense ca. 620-nm band and an axial EPR signal with a small hyperfine

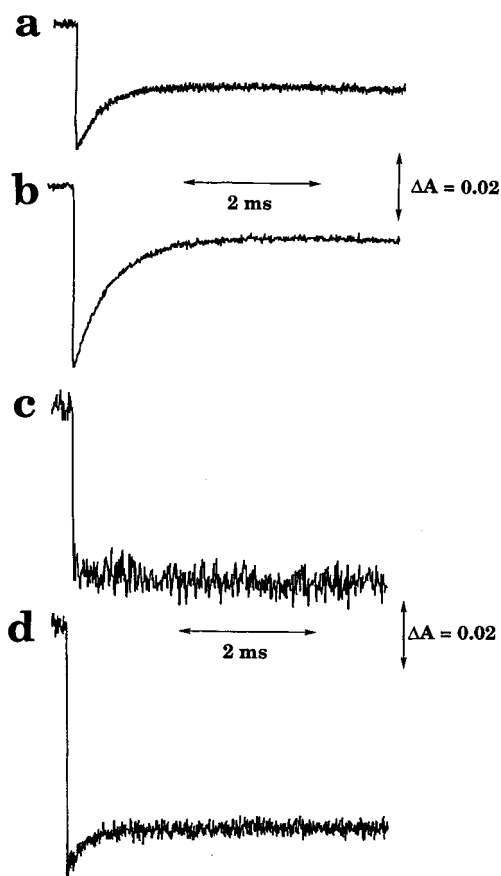


FIGURE 5. Time-resolved absorption changes of AxxNIR solution (pH 6.0) in the absence (a) and in the presence (b) of nitrite, and Asp98Ala solution (pH 7.0) in the absence (c) and in the presence (d) of nitrite at 20 °C.

coupling constant (A_0) of ca. 6 mT.⁴² Az was reported as an electron donor for the blue NIR from *Pseudomonas aureofaciens*³⁴ and AxxNIR.⁴³ However, the cyclic-voltammetric responses of the two Az's from Axx strain were slightly changed in the presence of AxxNIR and nitrite, indicating the very slow electron-transfer processes.²¹ Moreover, it has been shown by an *in vivo* approach with mutant strains of *Pseudomonas aeruginosa* deficient in one or both of cytochrome c_{551} (Cyt c_{551}) and Az that Cyt c_{551} , not Az, is functional as an electron donor for heme-containing NIR.⁴⁴ The rate constant of the electron transfer from Axx-Cyt c_{551} to AxxNIR was estimated to be $4.0 \times 10^5 \text{ M}^{-1} \text{ s}^{-1}$ at pH 6.0 and 25 °C.⁴⁵ Therefore, an electron donor protein for blue CuNIR would also be Cyt c_{551} .

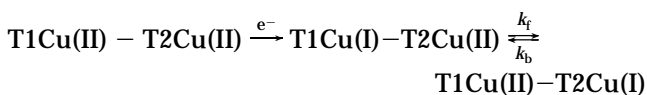
Intramolecular Electron-Transfer Process of CuNIR

The electron donated by an electron carrier at type 1 Cu is shifted to type 2 Cu, perhaps through the Cys136-His135 sequence segment (Figure 4). The intramolecular electron-transfer process was observed by pulse radiolysis.^{25,46–48} In Figure 5, traces a and b show time courses of the absorbances at 590 nm in the absence and in the presence of nitrite, respectively, after pulse radiolysis of AxxNIR.⁴⁷ In these absorption changes, the blue bands are quickly disappeared, indicating that the type 1 Cu sites are

Table 1. Observed Intramolecular Electron-Transfer Rate Constants (k_{ET}) of Native AxxNIR, Asp98Ala, and His255Ala in the Absence and in the Presence of Nitrite at pH 7.0 and 20 °C

AxxNIR and mutants (61–136 μM)	$k_{\text{ET}}/\text{s}^{-1}$
native AxxNIR	1900
native AxxNIR + nitrite (500 μM)	320
Asp98Ala	—
Asp98Ala + nitrite (500 μM)	3100
His255Ala	68
His255Ala + nitrite (500 μM)	113

reduced with a half-time period of ca. 10 μs. After the reduction of type 1 Cu, the slow recoveries of the absorbance at 590 nm are observed on the millisecond time scale. However, the corresponding absorbances of type 2 Cu-depleted (T2D) forms of AxxNIR and AciNIR do not recover even after 10 ms.^{25,46} A linear relationship between the amount of type 2 Cu in AciNIR and the recovered absorbance at 460 nm is observed.⁴⁶ These findings suggest that the recovery process is the intramolecular electron-transfer reaction from type 1 Cu (T1Cu) to type 2 Cu (T2Cu) as follows:



The observed intramolecular electron-transfer rate constant (k_{ET}) consists of the sum of k_f (forward) and k_b (backward). The k_{ET} values of AxxNIR in the absence and in the presence of nitrite were estimated to be $2 \times 10^3 \text{ s}^{-1}$ at pH 6.^{21,47} This value indicates a half-life period of 0.3 ms.

To shed light on a role of the hydrogen-bonding network containing Asp98 and His255 around the type 2 Cu center (Figure 4), two mutant AxxNIRs in which these amino acid residues are replaced with Ala were prepared. In Figure 5, traces c and d exhibit the absorption changes after pulse radiolysis of Asp98Ala in the absence and in the presence of nitrite at pH 7.0, respectively.⁴⁹ In the absence of nitrite, nonrecovery of the absorbance at 590 nm indicates that the electron-transfer process from type 1 Cu to type 2 Cu does not occur or is extremely slow. In the presence of nitrite, however, the recovery due to the electron-transfer process is observed. An increase of the absorbance is about 25% at 5 ms, although reoxidation of type 1 Cu in native AxxNIR occurs completely at the same time.⁴⁷ The k_{ET} value of Asp98Ala is, interestingly, larger than that of AxxNIR, as shown in Table 1.⁴⁹ The k_{ET} values of His255Ala in the absence and in the presence of nitrite are smaller than those of the native enzyme. These results imply that both the Asp98 and His255 residues around type 2 Cu control the intramolecular electron-transfer process by the formation of the hydrogen-bonding network. In addition to the role in the electron-transfer process, each of these amino acid residues would provide a proton for nitrite bonded to type 2 Cu in the nitrite reduction process (*vide infra*).

The pH dependence of k_{ET} of AciNIR in the absence and in the presence of nitrite is depicted in Figure 6.⁴⁷ The k_{ET} values independent of nitrite in the range of pH

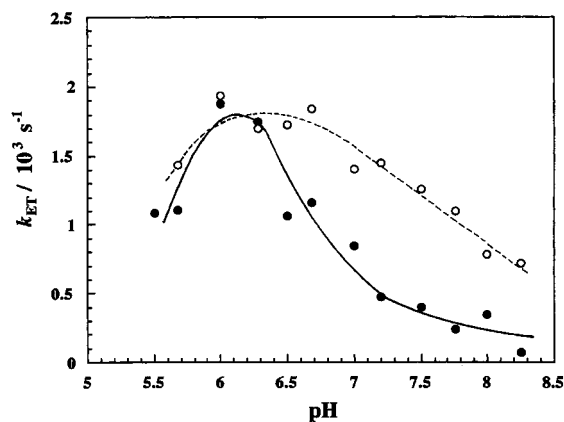


FIGURE 6. pH dependence of intramolecular electron-transfer rate constant (k_{ET}) of AciNIR in the absence (○) and in the presence (●) of nitrite at 20 °C.

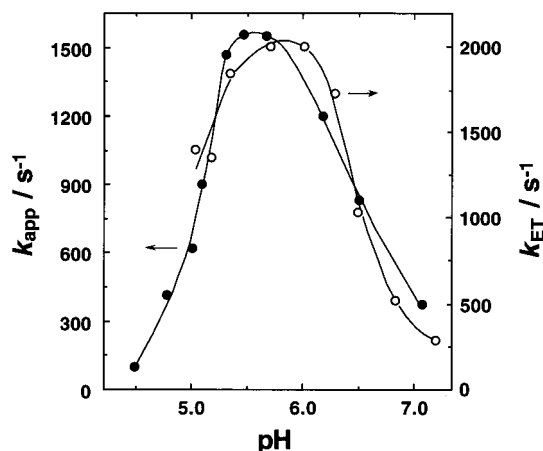


FIGURE 7. pH dependence of intramolecular electron-transfer rate constant (k_{ET}) of AxcNIR in the presence of nitrite and apparent catalytic rate constant (k_{app}) of AxcNIR.

5.5–6.3 show a maximum of $2 \times 10^3 \text{ s}^{-1}$ near pH 6. Above pH 6.3, the k_{ET} values in the absence of nitrite are decreased with increasing pH, whereas those in the presence of nitrite are abruptly decreased. The pH profile for k_{ET} of AxcNIR also presents a behavior similar to that of AciNIR⁴⁷ (see Figure 7). These results suggest that the binding of nitrite to type 2 Cu possibly brings about deprotonation of His255, forming the hydrogen-bonding network around type 2 Cu, that is, the cleavage of the network. This proposal might be supported by the fact that k_{ET} of His255Ala having no hydrogen-bonding network is considerably smaller than that of the native enzyme (Table 1).

The redox potentials of the type 1 and 2 Cu centers in AxcNIR and AciNIR were determined by cyclic voltammetry and pulse radiolysis. The type 1 Cu potential (+0.24 V vs NHE) of AciNIR is close to the +0.25-V midpoint potential of Aci-pAz at pH 7.0.⁴⁷ The midpoint potential (+0.20 V at pH 7.0) of T2D-AciNIR is slightly shifted to negative potential compared with that of native AciNIR.²⁵ The differences between two potentials of type 1 and 2 Cu's in AciNIR and AxcNIR are less than 50 mV.⁴⁷ Since the redox potential of type 2 Cu is shifted to more positive potential than that of type 1 Cu, the electron-transfer

process from type 1 Cu to type 2 Cu is energetically favored. On the other hand, the NIR from *Rhodobacter sphaeroides* 2.4.3 has the +0.247-V midpoint potential (type 1 Cu), and the type 2 Cu reduction potential is below +0.200 V in the absence of nitrite.⁵² Although reduction of type 2 Cu(II) by type 1 Cu(I) is not energetically favored, it is suggested that the binding of nitrite to type 2 Cu(II) is the trigger, positively shifting the type 2 Cu reduction potential, and induces the electron-transfer reaction.

Nitrite Reduction Process of CuNIR

Figure 7 shows the pH dependence of the catalytic activity of AxcNIR together with that of k_{ET} . The pH profile for k_{app} (apparent catalytic rate constant) is bell-shaped with the optimum near pH 5.5,³³ being substantially similar to those of AciNIR,²⁶ AfsNIR,³⁰ and AxcNIR.²⁴ The bell-shaped curve implies that two protonated groups with pK_a values of about 5 and 7 are involved in catalysis. The X-ray crystal structures of blue and green NIRs show that there are only two nonligand ionizable conserved residues around type 2 Cu, Asp98 and His255 (vide ante). Therefore, these residues are likely to be the immediate sources of the two protons utilized in the nitrite reduction. Steady-state kinetic analyses were performed with the Asp and His mutants of AxcNIR (Asp98Ala, Asp98Asn, Asp98Glu; His255Ala, His255Lys, His255Arg) to elucidate the roles of these residues.³³ In all Asp98 mutants, decreases by 2–3% of k_{app} of recombinant AxcNIR are observed at pH 5.5, and their apparent K_m values for nitrite are increased by factors of 17 (Asp98Glu), 65 (Asp98Ala), and 200 (Asp98Asn) compared with that of the recombinant AxcNIR. The K_m of Asp98Glu introducing the carboxyl group like Asp shows a little increase, indicating that hydrogen bond formation between the carboxyl group and nitrite would be necessary to anchor nitrite. The k_{app} values of three His255 mutants are 0.3–0.4% of that of the recombinant at pH 5.5, and their K_m values for nitrite are increased 23 (His255Ala), 5 (His255Lys), and 2 (His255Arg) times. The His287Glu mutant of RhsNIR also shows a similar decrease in catalytic activity (0.3% of the wild type) and unchanged K_m value.⁵² Therefore, His255 is not involved in nitrite binding directly but presumably controls the position of Asp98 through the hydrogen-bonding network. Moreover, the low catalytic activities of the His255 mutants as well as the Asp98 mutants supports that His255 also play the role of proton donor to nitrite bound to type 2 Cu. For the proton donation, the protonated imidazole (imidazolium) ring of His255 probably approaches to the substrate. According to X-ray crystal structure analysis, there is a vacancy in which this histidyl side chain is movable to approach type 2 Cu. Figure 8 depicts the proposed catalytic mechanism of CuNIR based on the X-ray crystal structures of native and nitrite-soaked CuNIRs¹³ and the kinetics of the Asp and His mutants.³³ In the first step, the substrate is replaced with the water ligand, which is released as OH^- (I → II). Type 2 Cu accepts one electron, and the NOOH interme-

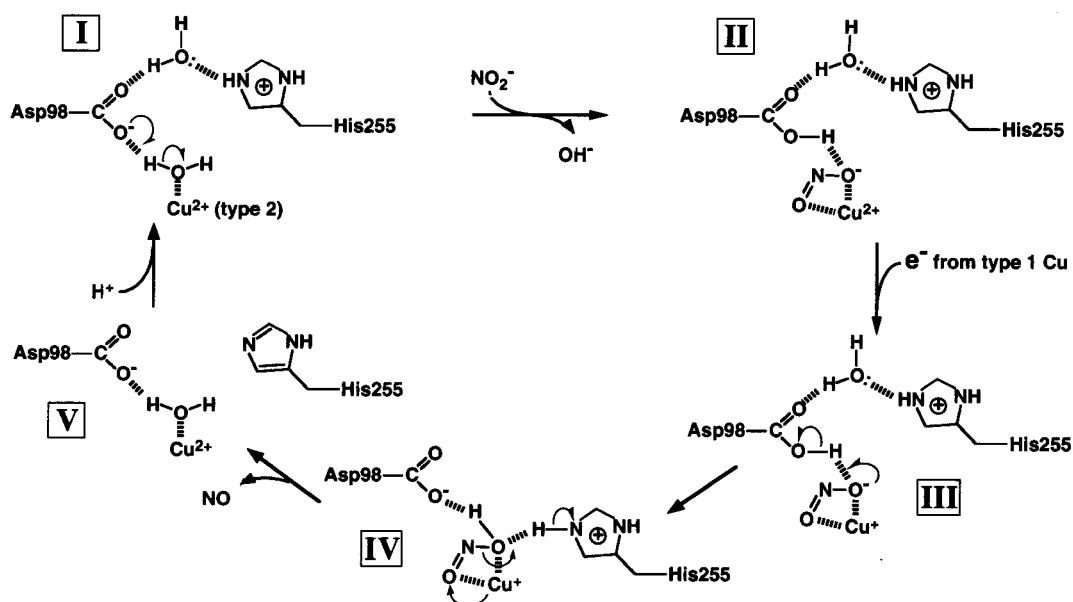


FIGURE 8. Proposed catalytic mechanism of CuNIR.

diolate is formed by protonation of nitrite (II \rightarrow III). The movement of protonated His255 toward the type 2 Cu site and the electron transfer from type 2 Cu(I) to NOOH may facilitate cleavage of the N–O bond (III \rightarrow IV). One proton would be donated from the His255 imidazolium group to produce a water ligand, and NO is generated (IV \rightarrow V). Asp98 and His255 residues behave as general acid–base catalysts, which provide two protons required for the substrate reduction (proton shuttling residues).

The pH profile for k_{app} is interestingly consistent that for k_{ET} , as shown in Figure 7. This means that the two amino acid residues, Asp98 and His255, would function in both the intramolecular electron-transfer and the catalytic processes, which will be closely associated with each other.

Conclusions

CuNIRs from denitrifying bacteria (*Alcaligenes xylosoxidans* GIFU 1051 and NCIB 11015 (blue NIR), *Achromobacter cycloclastes* IAM 1013, and *Alcaligenes faecalis* S-6 (green NIR)) are a homotrimer, and one subunit (ca. 36 kDa) contains each of type 1 Cu (two His, Cys, and Met ligands) and type 2 Cu (three His and solvent ligands). The type 1 Cu sites for accepting one electron in blue and green NIRs have distorted tetrahedral and flattened tetrahedral geometries, respectively. The type 2 Cu sites for catalyzing nitrite reduction in both NIRs are tetrahedral structures. The interatomic distance between the type 1 and 2 Cu's is 12.6 Å, and these Cu atoms are bound by the Cys–His sequence segment, which is probably the electron pathway from type 1 Cu to type 2 Cu. The intramolecular electron transfer occurs with a first-order electron-transfer rate constant (k_{ET}) of $2 \times 10^3 \text{ s}^{-1}$ at pH 6. In both NIRs, pH profiles for k_{ET} values are similar to those of the catalytic activities, indicating that the intramolecular electron-transfer process would be closely

linked to the following nitrite reduction process. Moreover, the intramolecular electron transfer and the catalytic kinetics of the Asp98 and His255 mutants demonstrate that each of Asp and His around the type 2 Cu site not only controls the electron-transfer process but also provides a proton for nitrite bound to type 2 Cu as a general acid–base catalyst in the nitrite reduction process.

The recent studies in our laboratory have been supported by Grants-in-Aid for Scientific Research on Priority Area (Nos. 08249221, 09235216, 10129217, 11116218) and Scientific Research (B) (No. 11440198) from the Ministry of Education, Science, Sports and Culture. We appreciate the advice and help of Dr. Kazuo Kobayashi and Prof. Seiichi Tagawa, the Institute of Scientific and Industrial Research, Osaka University, in the pulse radiolysis. We are grateful to Dr. Tsuyoshi Inoue and Prof. Yasushi Kai, Graduate School of Engineering, Osaka University, for X-ray crystal structure analysis. We also acknowledge Prof. Sohsuke Shidara (Faculty of Integrated Arts and Sciences, Hiroshima University) and Dr. Hidekazu Iwasaki for valuable discussions.

References

- (1) Smil, V. Global Population and the Nitrogen Cycle. *Sci. Am.* **1997**, July, 58–63.
- (2) Zumft, W. G. Cell Biology and Molecular Basis of Denitrification. *Microbiol. Mol. Biol. Rev.* **1997**, *61*, 533–616.
- (3) Averill, B. A. Dissimilatory Nitrite and Nitric Oxide Reductases. *Chem. Rev.* **1996**, *96*, 2951–2964.
- (4) Hille, R. The Mononuclear Molybdenum Enzymes. *Chem. Rev.* **1996**, *96*, 2757–2816.
- (5) Fulop, V.; Moir, J. W. B.; Ferguson, S. J.; Hajdu, J. The Anatomy of a Bifunctional Enzyme: Structural Basis for Reduction of Oxygen to Water and Synthesis of Nitric Oxide by Cytochrome *cd₁*. *Cell* **1995**, *81*, 369–377.
- (6) Nurizzo, D.; Silvestrini, M.-C.; Mathieu, M.; Cutruzzola, F.; Bourgeois, D.; Fulop, V.; Hajdu, J.; Brunori, M.; Tegoni, M.; Cambillau, C. N-Terminal Arm Exchange is Observed in the 2.15 Å Crystal Structure of Oxidized Nitrite Reductase from *Pseudomonas aeruginosa*. *Structure* **1997**, *5*, 1157–1171.
- (7) Baker, S. C.; Saunders, N. F. W.; Willis, A. C.; Ferguson, S. J.; Hajdu, J.; Fulop, V. Cytochrome *cd₁* Structure: Unusual Haem Environments in a Nitrite Reductase and Analysis of Factors Contributing to β -Propeller Folds. *J. Mol. Biol.* **1997**, *269*, 440–455.

- (8) Godden, J. W.; Turley, S.; Teller, C.; Adman, E. T.; Liu, M. Y.; Payne, W. J.; LeGall, P. J. The 2.3 Å Structure of Nitrite Reductase from *Achromobacter cycloclastes*. *Science* **1991**, *253*, 438–442.
- (9) Kukimoto, M.; Nishiyama, M.; Murphy, M. E.; Turley, S.; Adman, E. T.; Horinouchi, S.; Beppu, T. X-ray Structure and Site-directed Mutagenesis of a Nitrite Reductase from *Alcaligenes faecalis* S-6: Roles of Two Copper Atoms in Nitrite Reductase. *Biochemistry* **1994**, *33*, 5246–5252.
- (10) Murphy, M. E. P.; Turley, S.; Kukimoto, M.; Nishiyama, M.; Horinouchi, S.; Sasaki, H.; Tanokura, M.; Adman, E. T. Structure of *Alcaligenes faecalis* Nitrite Reductase and A Copper Site Mutant, M150E, That Contains Zinc. *Biochemistry* **1995**, *34*, 12107–12117.
- (11) Adman, E. T.; Godden, J. W.; Turley, S. The Structure of Copper-Nitrite Reductase from *Achromobacter cycloclastes* at Five pH Values with NO₂⁻ Bound and with Type II Copper Depleted. *J. Biol. Chem.* **1995**, *270*, 27458–27474.
- (12) Strange, R. W.; Dodd, F. E.; Abraham, Z. H. L.; Grossmann, J. G.; Bruser, T.; Eady, R. R.; Smith, B. E.; Hasnain, S. S. The Substrate-binding Site in Cu Nitrite Reductase and Its Similarity to Zn Carbonic Anhydrase. *Nature Struct. Biol.* **1995**, *2*, 287–292.
- (13) Murphy, M. E. P.; Turley, S.; Adman, E. T. Structure of Nitrite Bound to Copper-Containing Nitrite Reductase from *Alcaligenes faecalis*. *J. Biol. Chem.* **1997**, *272*, 28455–28460.
- (14) Inoue, T.; Gotowda, M.; Deligeer, K.; Kataoka, K.; Yamaguchi, K.; Suzuki, S.; Watanabe, H.; Gohow, M.; Kai, Y. Type I Cu Structure of Blue Nitrite Reductase from *Alcaligenes xylosoxidans* GIFU 1051 at 2.05 Å Resolution: Comparison of Blue and Green Nitrite Reductase. *J. Biochem.* **1998**, *124*, 876–879.
- (15) (a) Dodd, F. E.; Hasnain, S. S.; Abraham, Z. H. L.; Eady, R. R.; Smith, B. E. Structures of a Blue-Copper Nitrite Reductase and Its Substrate-Bound Complex. *Acta Crystallogr.* **1997**, *D53*, 406–418. (b) Dodd, F. E.; Van Beeumen, J.; Eady, R. R.; Hasnain, S. S. X-ray Structure of a Blue-Copper Nitrite Reductase in Two Crystal Forms. The Nature of the Copper Sites, Mode of Substrate Binding and Recognition by Redox Partners. *J. Mol. Biol.* **1998**, *282*, 369–382.
- (16) Strange, R. W.; Murphy, L. M.; Dodd, F. E.; Abraham, Z. H. L.; Eady, R. R.; Smith, B. E.; Hasnain, S. S. Structural and Kinetic Evidence for an Ordered Mechanism of Copper Nitrite Reductase. *J. Mol. Biol.* **1999**, *287*, 1001–1009.
- (17) Sakurai, N.; Sakurai, T. Isolation and Characterization of Nitric Oxide Reductase from *Paracoccus halodenitrificans*. *Biochemistry* **1997**, *36*, 13809–13815.
- (18) Brown, K.; Tegoni, M.; Prudencio, M.; Pereira, A. S.; Besson, S.; Moura, J. J.; Moura, I.; Cambillau, C. A Novel Type of Catalytic Copper Cluster in Nitrous oxide Reductase. *Nature Struct. Biol.* **2000**, *7*, 191–195.
- (19) Tsukihara, T.; Aoyama, H.; Yamashita, E.; Tomizuka, T.; Yamaguchi, H.; Shinzawa-Itoh, K.; Nakashima, R.; Yano, R.; Yoshikawa, S. Structures of Metal Sites of Oxidized Bovine Heart Cytochrome c Oxidase at 2.8 Å. *Science* **1995**, *269*, 1069–1074.
- (20) Iwata, S.; Ostermeier, C.; Ludwig, B.; Michel, H. Structure at 2.8 Å Resolution of Cytochrome c Oxidase from *Paracoccus denitrificans*. *Nature* **1995**, *376*, 660–669.
- (21) Suzuki, S.; Kataoka, K.; Yamaguchi, K.; Inoue, T.; Kai, Y. Structure-Function Relationships of Copper-containing Nitrite Reductases. *Coord. Chem. Rev.* **1999**, *190–192*, 245–265.
- (22) Masuko, M.; Iwasaki, H.; Sakurai, T.; Suzuki, S.; Nakahara, A. Characterization of Nitrite Reductase from a Denitrifier, *Alcaligenes* sp. NCIB 11015. A Novel Copper Protein. *J. Biochem.* **1984**, *96*, 447–454.
- (23) Abraham, Z. H. L.; Lowe, D. J.; Smith, B. E. Purification and Characterization of the Dissimilatory Nitrite Reductase from *Alcaligenes xylosoxidans* subsp. *xylosoxidans* (N.C.I.M.B. 11015): Evidence for the Presence of Both Type 1 and Type 2 Copper Centres. *Biochem. J.* **1993**, *295*, 587–593.
- (24) Abraham, Z. H. L.; Smith, B. E.; Howes, B. D.; Lowe, D. J.; Eady, R. R. pH-Dependence for Binding a Single Nitrite Ion to Each Type-2 Copper in the Copper-Containing Nitrite Reductase of *Alcaligenes xylosoxidans*. *Biochem. J.* **1997**, *324*, 511–516.
- (25) Suzuki, S.; Deligeer, Y.; Yamaguchi, K.; Kataoka, K.; Kobayashi, K.; Tagawa, S.; Kohzuma, T.; Shidara, S.; Iwasaki, H. Spectroscopic Characterization and Intramolecular Electron Transfer Process of Native and Type 2 Cu-Depleted Nitrite Reductase. *J. Biol. Inorg. Chem.* **1997**, *2*, 265–274.
- (26) Iwasaki, H.; Matsubara, T. A Nitrite Reductase from *Achromobacter cycloclastes*. *J. Biochem.* **1972**, *71*, 645–652.
- (27) Liu, M.-Y.; Liu, M.-C.; Payne, W. J.; LeGall, J. Properties and Electron Transfer Specificity of Copper Proteins from the Denitrifier "*Achromobacter cycloclastes*". *J. Bacteriol.* **1986**, *166*, 604–608.
- (28) Suzuki, S.; Yoshimura, T.; Kohzuma, T.; Masuko, M.; Sakurai, T.; Iwasaki, H. Spectroscopic Evidence for a Copper-Nitrosyl Intermediate in Nitrite Reduction by Blue Copper-Containing Nitrite Reductase. *Biochem. Biophys. Res. Commun.* **1989**, *164*, 1366–1372.
- (29) Libby, E.; Averill, B. A. Evidence That the Type 2 Copper Centers Are the Site of Nitrite Reduction by *Achromobacter cycloclastes* Nitrite Reductase. *Biochem. Biophys. Res. Commun.* **1992**, *187*, 1529–1535.
- (30) Kakutani, T.; Watanabe, H.; Arima, K.; Beppu, T. Purification and Properties of a Copper-Containing Nitrite Reductase from a Denitrifying Bacterium, *Alcaligenes faecalis* Strain S-6. *J. Biochem.* **1981**, *89*, 453–461.
- (31) LaCroix, L. B.; Shadle, S. E.; Wang, Y.; Averill, B. A.; Hedman, B.; Hodgson, K. O.; Solomon, E. Electronic Structure of the Perturbed Blue Copper Site in Nitrite Reductase: Spectroscopic Properties, Bonding, and Implications for the Entatic/Rack State. *J. Am. Chem. Soc.* **1996**, *118*, 7755–7768.
- (32) Suzuki, E.; Horikoshi, N.; Kohzuma, T. Cloning, Sequencing, and Transcriptional Studies of the Gene Encoding Copper-Containing Nitrite Reductase from *Alcaligenes xylosoxidans* NCIMB 11015. *Biochem. Biophys. Res. Commun.* **1999**, *255*, 427–431.
- (33) Kataoka, K.; Furusawa, H.; Takagi, K.; Yamaguchi, K.; Suzuki, S. Functional Analysis of Conserved Aspartate and Histidine Residues Located Around the Type 2 Copper Site of Copper-Containing Nitrite Reductase. *J. Biochem.* **2000**, *127*, 345–350.
- (34) Zumft, W. G.; Gotzmann, D. J.; Kroneck, P. M. H. Type 1, Blue Copper Proteins Constitute a Respiratory Nitrite-Reducing System in *Pseudomonas aureofaciens*. *Eur. J. Biochem.* **1987**, *168*, 301–307.
- (35) Iwasaki, H.; Matsubara, T. Purification and Some Properties of *Achromobacter cycloclastes* Azurin. *J. Biochem.* **1973**, *73*, 659–661.
- (36) Kukimoto, M.; Nishiyama, M.; Ohnuki, T.; Turley, S.; Adman, E. T.; Horinouchi, S.; Beppu, T. Identification of Interaction Site of Pseudoazurin with Its Redox Partner, Copper-Containing Nitrite Reductase from *Alcaligenes faecalis* S-6. *Protein Eng.* **1995**, *8*, 153–158.
- (37) Kohzuma, T.; Dennison, C.; McFarlane, W.; Nakashima, S.; Kitagawa, T.; Inoue, T.; Kai, Y.; Nishio, N.; Shidara, S.; Suzuki, S.; Sykes, A. G. Spectroscopic and Electrochemical Studies on Active-site Transitions of the Type 1 Copper Protein Pseudoazurin from *Achromobacter cycloclastes*. *J. Biol. Chem.* **1995**, *270*, 25733–25738.
- (38) Kohzuma, T.; Takase, S.; Shidara, S.; Suzuki, S. Electrochemical Properties of Copper Proteins, Pseudoazurin and Nitrite Reductase from *Achromobacter cycloclastes* IAM 1013. *Chem. Lett.* **1993**, 149–152.
- (39) Adman, E. T.; Turley, S.; Bramson, R.; Petratos, K.; Banner, D.; Tsernoglou, D.; Beppu, T.; Watanabe, H. A 2.0-Å Structure of the Blue Copper Protein (Cupredoxin) from *Alcaligenes faecalis* S-6. *J. Biol. Chem.* **1989**, *264*, 87–99.
- (40) Inoue, T.; Nishio, N.; Suzuki, S.; Kataoka, K.; Kohzuma, T.; Kai, Y. Crystal Structure Determinations of Oxidized and Reduced Pseudoazurins from *Achromobacter cycloclastes*. *J. Biol. Chem.* **1999**, *274*, 17845–17852.
- (41) Kukimoto, M.; Nishiyama, M.; Tanokura, M.; Adman, E. T.; Horinouchi, S. Studies on Protein-protein Interaction between Copper-Containing Nitrite Reductase and Pseudoazurin from *Alcaligenes faecalis* S-6. *J. Biol. Chem.* **1996**, *271*, 13680–13688.
- (42) Yamaguchi, K.; Nakamura, N.; Shidara, S.; Iwasaki, H.; Suzuki, S. Isolation Characterization of Two Distinct Azurins from *Alcaligenes xylosoxidans* subsp. *xylosoxidans* NCIB11015 or GIFU 1051. *Chem. Lett.* **1995**, 353–354.
- (43) Dodd, F. E.; Hasnain, S. S.; Hunter, W. N.; Abraham, Z. H. L.; Debenham, M.; Kanzler, H.; Eldridge, M.; Eady, R. R.; Ambler, R. P.; Smith, B. E. Evidence for Two Distinct Azurins in *Alcaligenes xylosoxidans* (NCIMB 11015): Potential Electron Donors to Nitrite Reductase. *Biochemistry* **1995**, *34*, 10180–10186.
- (44) Vijgenboom, E.; Julie, E.; Busch, E.; Canters, G. W. *In Vivo* Studies Disprove an Obligatory Role of Azurin in Denitrification in *Pseudomonas aeruginosa* and Show That Azu Expression Is under Control of RpoS and ANR. *Microbiology* **1997**, *143*, 2853–2863.
- (45) Deligeer, Y.; Kataoka, K.; Yamaguchi, K.; Suzuki, S. Spectroscopic and Electrochemical Properties of Cytochrome c₅₅₁ from *Alcaligenes xylosoxidans* GIFU 1051. *Bull. Chem. Soc. Jpn.* **2000**, *73* (8), in press.
- (46) Suzuki, S.; Kohzuma, T.; Deligeer, Y.; Yamaguchi, K.; Nakamura, N.; Shidara, S.; Kobayashi, K.; Tagawa, S. Pulse Radiolysis Studies on Nitrite Reductase from *Achromobacter cycloclastes* IAM

- 1013: Evidence for Intramolecular Electron Transfer from Type 1 Cu to Type 2 Cu. *J. Am. Chem. Soc.* **1994**, *116*, 11145–11146.
- (47) Kobayashi, K.; Tagawa, S.; Deligeer; Suzuki, S. The pH-Dependence Changes of Intramolecular Electron Transfer on Copper-Containing Nitrite Reductase. *J. Biochem.* **1999**, *126*, 408–412.
- (48) Farver, O.; Eady, R. R.; Abraham, Z. H. L.; Pecht, I. The Intramolecular Electron Transfer between Copper Sites of Nitrite Reductase: A Comparison with Ascorbate Oxidase. *FEBS Lett.* **1998**, *436*, 239–242.
- (49) Suzuki, S.; Furusawa, H.; Kataoka, K.; Yamaguchi, K.; Kobayashi, K.; Tagawa, S. Intramolecular Electron Transfer Process of Native and Mutant Forms of Blue Copper-Containing Nitrite Reductase from *Alcaligenes xylooxidans*. *Inorg. React. Mech.*, in press.
- (50) Kohzuma, T.; Shidara, S.; Suzuki, S. Direct Electrochemistry of Nitrite Reductase from *Achromobacter cycloclastes* IAM 1013. *Bull. Chem. Soc. Jpn.* **1994**, *67*, 138–143.
- (51) Kohzuma, T.; Shidara, S.; Yamaguchi, K.; Nakamura, N.; Deligeer; Suzuki, S. Direct Electrochemistry of Copper-Containing Nitrite Reductase from *Achromobacter xylooxidans* NCIB 11015. *Chem. Lett.* **1993**, 2029–2032.
- (52) Olesen, K.; Veselov, A.; Zhao, Y.; Wang, B.; Danner, B.; Scholes, C. P.; Shapleigh, J. P. Spectroscopic, Kinetic, and Mutant forms of Copper-Containing Nitrite Reductase from *Rhodobacter sphaeroides* 2.4.3. *Biochemistry* **1998**, *37*, 6086–6094.

AR9900257